PHYSICAL REVIEW LETTERS **129,** 140402 (2022)

Editors' Suggestion   Featured in Physics

Emergence of Fermi's Golden Rule

Tobias Micklitz,[1] Alan Morningstar,[2] Alexander Altland,[3] and David A. Huse[2,4]

[1]*Centro Brasileiro de Pesquisas Físicas, Rua Xavier Sigaud 150, 22290-180 Rio de Janeiro, Brazil*
[2]*Department of Physics, Princeton University, Princeton, New Jersey 08544, USA*
[3]*Institut für Theoretische Physik, Universität zu Köln, Zülpicher Strasse 77, 50937 Cologne, Germany*
[4]*Institute for Advanced Study, Princeton, New Jersey 08540, USA*

(Received 13 June 2022; accepted 18 August 2022; published 27 September 2022)

Fermi's golden rule applies in the limit where an initial quantum state is weakly coupled to a *continuum* of other final states overlapping its energy. Here we investigate what happens away from this limit, where the set of final states is discrete, with a nonzero mean level spacing; this question arises in a number of recently investigated many-body systems. For different symmetry classes, we analytically and/or numerically calculate the universal crossovers in the average decay of the initial state as the level spacing is varied, with the golden rule emerging in the limit of a continuum. Among the corrections to the exponential decay of the initial state given by Fermi's golden rule is the appearance of the spectral form factor in the longtime regime for small but nonzero level spacing.

DOI: 10.1103/PhysRevLett.129.140402

Introduction and motivation.—Fermi's golden rule (FGR) describes the decay of an initial state into a continuum of final states [1–3]. To have a true continuum of final states we would need to have an infinite system, such as an excited atom emitting a photon into an infinite vacuum. What happens if, instead, the set of final states is discrete, with some nonzero average energy-level spacing? This question, which is addressed in the present Letter, arises in multiple contexts in the study of the quantum dynamics of isolated many-body systems.

When considering the thermalization of a finite-size isolated many-body quantum system, we ask, Does this system act as a "bath" for its own degrees of freedom? As a finite-size system, it cannot be a perfect bath, since it has a discrete spectrum. Two limiting situations are rather clear. If the energy-level spacing in the putative bath is large compared to the matrix elements coupling our initial state to these final states, then the initial state typically has no final states to decay to that are close enough to on shell, so the initial state typically does not decay. The opposite limit is where Fermi's golden rule does apply, because the decay rate of the initial state is large compared to the energy-level spacing of the final states, so the discrete spectrum serves as a good approximation to a continuum. In the present Letter we analytically calculate the intermediate behavior between these two limits for a single initial quantum state coupled to a chaotic quantum dot modeled by a random matrix of large dimension N and show numerical results in full agreement with those calculations.

The above considerations have become increasingly important recently, in an era where controlled and detailed access to mesoscopic quantum many-body systems is a reality [4–6]. Such systems can have states that may decay into sets of other states of the system, depending on the degree to which an approximate continuum is formed for the relevant decay processes. Manifestations of this physics, to be discussed further near the end of this Letter, include the crossover or transition at the onset of heating in periodically driven (Floquet) systems [7–9], "avalanche" instabilities of many-body localization (MBL) in systems with short-range interactions [10–12], the Fock-space localization description of the onset of many-body quantum chaos in finite-size MBL systems with long-range interactions [13–17], and finite-size systems with weakly broken integrability [18–20]. Our Letter is also related to previous investigations of the thermalization of single spins coupled weakly to finite quantum systems [21,22], and to studies of decay and recurrences in other solvable models of a discrete set of levels coupled to a (quasi)continuum [23–25].

In the following we will define a concrete level-dot model to use in exploring various qualitative and universal deviations from golden-rule behavior. This also reveals how FGR behavior emerges from the behavior of finite systems with discrete spectra, as the limit of a continuous spectrum is approached. A more general two-dot model is discussed in Supplemental Material [26]. The two dots may represent two states of a weakly coupled spin.

Model and observable.—Consider a single level $|0\rangle$ weakly coupled to the $N \gg 1$ levels $\{|\mu\rangle\}_{\mu=1,\ldots,N}$ of a fully chaotic quantum dot. We first assume that time-reversal symmetry is broken, and model the system by the random matrix Hamiltonian,

$$\hat{\mathcal{H}} = \sum_{\mu,\nu=0}^{N} |\mu\rangle \begin{pmatrix} \epsilon_0 & W \\ W^\dagger & H \end{pmatrix}_{\mu\nu} \langle\nu|, \qquad (1)$$

where H and W are a random Hermitian $N \times N$ matrix and an N-component vector of independently distributed complex variables, respectively. The matrix elements have zero mean and variances $\langle H_{kl} H^*_{mn} \rangle_H = (\lambda^2/N)\delta_{km}\delta_{ln}$ and $\langle W_k W^*_l \rangle_W = (g\lambda^2/N)\delta_{kl}$, and we assume $\epsilon_0 = 0$, so the initial state resides at the band center of the dot states. The spectrum of H forms the Wigner semicircle [28], with the density of states at its band center being $\nu = (N/\pi\lambda)$. Below, we will also generalize to cases where time-reversal symmetry remains unbroken.

To study the decay of the initial state $|0\rangle$, we consider the average of the time-dependent probability to stay in that state:

$$P(t) = \langle |\langle 0|0(t)\rangle|^2 \rangle_{H,W}. \tag{2}$$

Averages $\langle \cdots \rangle_{H,W}$ here are over the random components of H and W, and $|0(t)\rangle = e^{-i\hat{\mathcal{H}}t}|0\rangle$ is the time-evolved initial state. Before turning to concrete calculations, let us formulate some qualitative anticipations.

In the case where we assume the quantum dot is a perfect bath, Fermi's golden rule gives the decay $P(t) \sim e^{-\Gamma_{\mathrm{FGR}}|t|}$ with the realization-averaged decay rate

$$\Gamma_{\mathrm{FGR}} = 2\pi \langle W_l W^*_l \rangle_W \nu = 2g\lambda. \tag{3}$$

The above result predicts a vanishing longtime "probability of residence" $P_{\mathrm{res}} \equiv P(t \to \infty) = 0$. However, this result cannot completely describe the decay of $|0\rangle$ into a system of finite dimension N: If the level-dot coupling is strong, e.g., $g = 1$, the longtime state $|0(t \to \infty)\rangle$ will be spread over the joint level-dot Hilbert space of dimension $N + 1 \approx N$, i.e., there is a lower bound $P_{\mathrm{res}} \approx 1/N$, different from zero. For a diminished coupling, $g < 1$, the level broadens to mix with only about $\Gamma_{\mathrm{FGR}}\nu \sim gN$ of the dot levels, so we anticipate an enhanced probability of residence $P_{\mathrm{res}} \sim 1/(gN)$. Further diminishing the coupling down to $g \sim O(N^{-1})$ leads into a regime where the effects due to the nonzero dot-level spacing become strong, and ultimately to a limit where only rare realizations have a dot level in resonant contact with the initial state. In the process, FGR breaks down, and P_{res} approaches unity.

Stationary limit.—To quantitatively describe this phenomenon, we have applied nonperturbative methods of (effective) matrix theory [26]. The result reads

$$P_{\mathrm{res}} = 1 - \gamma - \sqrt{\pi\gamma}\left(\frac{1}{2} - \gamma\right) e^{\gamma} \mathrm{erfc}(\sqrt{\gamma}), \tag{4}$$

with $\gamma \equiv gN$ and $\mathrm{erfc}(x) = (2/\sqrt{\pi}) \int_x^\infty dx e^{-x^2}$ the complementary error function. The limits $N \to \infty$ and $g \to 0$ have been taken jointly such that γ remains finite. This formula [see the gray curve in Fig. 2(d)] indeed predicts a crossover from the golden-rule estimate $P_{\mathrm{res}} = 1/\gamma = 1/gN$ for $\gamma > 1$ (the purple curve) to a fully decoupled level, $P_{\mathrm{res}} = 1$, at $\gamma \to 0$. The blue dots are results obtained via numerical diagonalization for matrices of size $N + 1 = 10^3$, averaged over 10^4 samples, and are in excellent agreement with our analytic result [29].

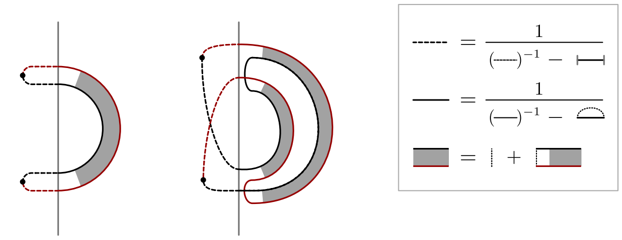

FIG. 1. Diagrammatic representation of the short-time ($\tau < 1$) correction to the FGR exponential decay of the initial state. Left-hand diagram (one ladder): classical probability that a particle, escaped into the dot, returns to the weakly coupled level. Right-hand diagram (two ladders): quantum interference correction to classical return probability. Dashed and solid lines here represent the retarded (black) or advanced (red) level and dot Green's functions $G_i^{\pm}(\epsilon) \sim (\epsilon - \epsilon_i \pm i\Sigma_i)^{-1}$, dressed by self-consistently calculated self-energies $\Sigma_0 \sim g\lambda$ and $\Sigma_\mu \sim \lambda$, as indicated in the box. The ladder defines the ergodic quantum dot mode $D(\omega) \sim i\lambda^2/(N\omega^+)$, and is recursively defined in the third equation in the box. The solid vertical line represents the coupling between $|0\rangle$ and quantum dot states. See also the Supplemental Material for further details and a nonperturbative calculation addressing all times, including $\tau > 1$ [26].

Dynamics.—We next turn to the interesting question of how the above longtime limits are dynamically approached. Before turning to the quantitative computation of $P(t)$, let us discuss some estimates based on perturbation theory applied to the quantum mechanical propagator $\mathcal{P}(t) = \langle 0|0(t)\rangle = \langle 0|e^{-i\hat{\mathcal{H}}t}|0\rangle$ of the level. In the joint limits $\gamma \to \infty$, $g \to 0$, $\mathcal{P}(t)$ is structureless, except for incoherent FGR decay due to coupling to the dot continuum. Substituting the broadened amplitude into Eq. (2), we obtain the zeroth-order result whose Fourier transform is $P_0(\omega) \sim 1/(\omega + 2ig\lambda)$. However, for finite N, coherent processes involving the propagation of the retarded amplitude $\mathcal{P}(t)$ and its advanced complex conjugate along identical dot-scattering paths begin to play a role (see Fig. 1 for the first two corrections of this type). While these processes are small in phase volume, $\sim N^{-1}$, each introduces a factor in time t indicating that the effective parameter of the perturbative analysis is $\tau \equiv t/(2\pi\nu) \sim t\lambda/N$. Referring to the Supplemental Material for details, the first-order process yields the contribution $P_1(\omega) \sim i/(gN\omega)$, where the frequency dependence $\omega^{-1} \to \Theta(t)$ reflects the ergodicity of the dot propagation on long time scales [26]. To second order, $P_2(\omega) \sim -\lambda/[g(N\omega)^2]$, and higher-order perturbative contributions do not exist (in the absence of time reversal; see below). Fourier transformation to the time domain yields initial exponential time dependence $P_0(\tau)$, cut off by a constant value $P_1(\tau) \equiv P_{\mathrm{off}}$, followed by a linear increase

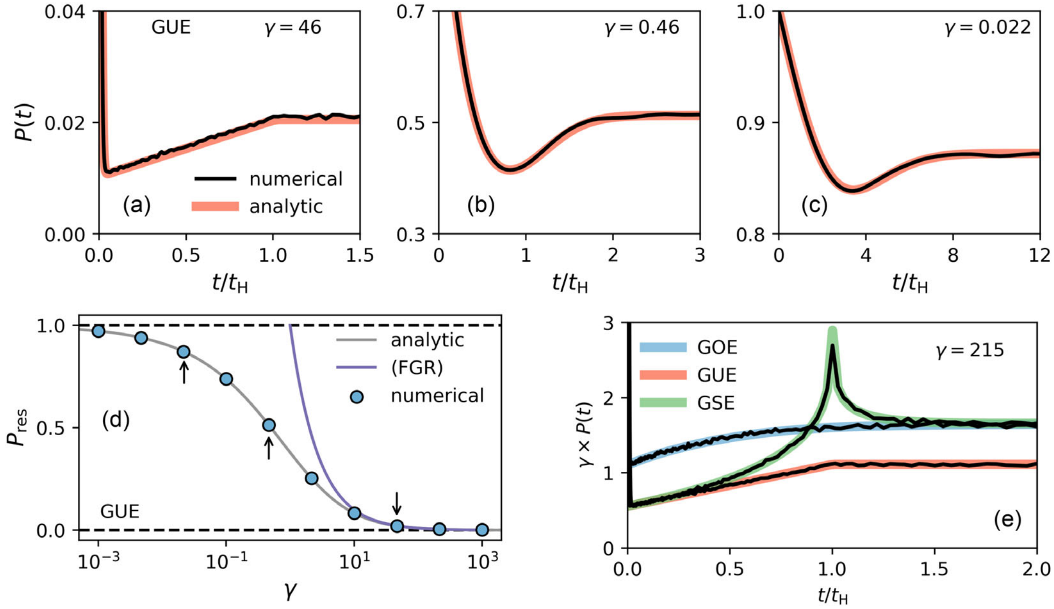

FIG. 2. The probability $P(t)$ to be in the initial state after time t. The total Hilbert space dimension is $N + 1 = 10^3$ and numerical data are averaged over 10^4 samples. (a)–(c) The time dependence of $P(t)$ for $\gamma \in \{46, 0.46, 0.022\}$, respectively. The black curves are data from numerical simulations of the model Eq. (1). The red curves are theoretical predictions obtained by evaluating the integral in Eq. (5) numerically. (d) The $t \to \infty$ limit P_{res}. Blue dots are numerical data. The gray curve is the theoretical prediction of Eq. (4). The purple curve is the FGR result $1/\gamma$ [29]. The small black arrows point to data that correspond to the late-time limits of the three upper panels. (e) The spectral form factor arises in the time dependence of $P(t)$ for the three versions of our model derived from the three Wigner-Dyson classes (GOE, GUE, GSE). The black curves are data from numerics, and the colored curves are Eq. (6) with parameters a_X and b_X as given in the main text. In panels (a)–(d) H is GUE.

$P_2(\tau) \sim \tau$. We thus observe *nonmonotonic* dependence of the probability $P(\tau)$, where an initial fast exponential decay is followed by an extended period of slow partial recovery. The resemblance of this temporal profile to that of the spectral form factor of random matrix theory [30] suggests that the late-time increase of $P(\tau)$ will saturate at a plateau $P(\tau) \sim (gN)^{-1}$ for $\tau > 1$. However, at this stage we are probing times $t \sim \nu$ of the order of the inverse average level spacing, outside the regime of perturbation theory.

The above discussion suggests that the discreteness of the level spacing is felt in two different ways: saturation of $P(t)$ at times beyond the Heisenberg time, $t_H = 2\pi\nu$, and the recovery of $P_{res} \sim 1$ for small coupling $\gamma \lesssim 1$. To quantitatively describe these phenomena, we apply nonperturbative methods of (effective) matrix theory (see Refs. [26,31]). The idea of this approach is to trade the complexity of an integral over the high-dimensional random matrices modeling the dot for a simpler one over a four-dimensional (super)matrix. The symmetry of the problem affords a further reduction to an integral over just two "radial coordinates," leading to our main analytic result,

$$P(\tau) = e^{-4\gamma\tau} + 2\gamma^2 \int_{-1}^{1} d\lambda_f \int_{1}^{\infty} d\lambda_b \frac{x^2 e^{-2\gamma x \lambda_b}}{\lambda_b - \lambda_f} \times [\lambda_b I_0(z_b) - \mu_b I_1(z_b)]\Theta(x), \tag{5}$$

where $x = x(\lambda_f, \lambda_b, \tau) = 2\tau - \lambda_b + \lambda_f$, $z_b = 2\gamma x \mu_b$, with $\mu_b = \sqrt{\lambda_b^2 - 1}$, and I_k are modified Bessel functions of the first kind. This expression captures the universal longtime deviations from FGR for finite γ. For finite N there will also be nonuniversal short-time deviations set by ultraviolet details.

For large $\gamma \gg 1$, an approximate evaluation of the integral leads to $P(\tau) = e^{-4\gamma\tau} + (1/2\gamma)(1+\tau)\Theta(1-\tau) + (1/\gamma)\Theta(\tau-1)$, where the first two terms recover the results of our previous perturbative estimate, and the third adds the expected saturation at a plateau value. The numerical evaluation of the full integral is shown in Figs. 2(a)–2(c) for values $\gamma = 46$, 0.46, and 0.022 (red curves). Comparison to numerical diagonalization of Eq. (1) with a total of 10^3 levels shows excellent agreement. These curves contain the main results of our analysis: for all coupling strengths, we observe initial decay followed by a slow partial recovery of $P(t)$, which eventually terminates in a stationary plateau. Diminishing the coupling leads to a rounding of the temporal profile, and to an increase in the stationary probability with a limiting value predicted by Eq. (4).

We finally mention one more universal signature of the profile $P(t)$, namely, a factor of 2 between the minimum P_{off} and the plateau (longtime residence) value $P_{pl} = P_{res} = 2P_{off}$ in the regime $\gamma \gg 1$. This universal ratio is remarkable inasmuch as it connects an early time semiclassical probability with a deep quantum signature depending on the discreteness of the spectrum. In the limits $N \gg \gamma \gg 1$, the semiclassical calculation yields $P_{\mathrm{off}} = 1/(2\gamma)$. The connection to P_{pl} follows from a formal decomposition of $P(t) = \sum_{\alpha\beta} |\psi_{\alpha,0}|^2 |\psi_{\beta,0}|^2 e^{i(\epsilon_\alpha - \epsilon_\beta)t}$ in eigenfunctions. For times exceeding the inverse level spacing, $\tau > 1$, only the coherent diagonal sum $\alpha = \beta$ contributes. Noting that eigenfunctions of chaotic systems behave as Gaussian distributed random variables, we obtain $P(t) \to P_{\mathrm{pl}} = \sum_\alpha |\psi_{\alpha,0}|^4 \approx 1/\gamma$, twice as high as the semiclassical value due to constructive quantum interference.

Time-reversal symmetry.—While the exponential decay at short times does not depend on symmetries, later stages of the dynamics do. Distinguishing between the three cases $T = (0, 1, -1) \equiv (\mathrm{U}, \mathrm{O}, \mathrm{S})$ of broken time-reversal invariance (U), and time-reversal invariance with (O) or without (S) spin rotation invariance, we note that for O, the semiclassical probability to return to the initial quantum state $|0\rangle$ doubles due to weak localization—i.e., constructive interference between a returning path and its time reverse. No such doubling occurs for S, because in this case the time-reversed amplitude ends up in a spin reversed state that is different from the initial state. We thus expect $P_{\mathrm{off}} = (1, 2, 1)/(2\gamma)$. Turning to the asymptotic plateau value, wave functions in the presence of time reversal (O and S) can be chosen real, and on this basis we expect $P_{\mathrm{pl}} = (2, 3, 3)/(2\gamma)$. This leads to a generalization of the universal ratios as $P_{\mathrm{pl}}/P_{\mathrm{off}} = (2, 3/2, 3)$. To understand the temporal profile at intermediate times, we suggest the generalization of $P(t)$ at coupling $\gamma \gg 1$ to be

$$P_X(\tau) = e^{-4\gamma\tau} + \frac{1}{2\gamma}[a_X + b_X K_X(\tau)], \qquad X \in \{\mathrm{U}, \mathrm{O}, \mathrm{S}\}, \tag{6}$$

i.e., a sum of incoherent decay, semiclassical return probability, and a slow partial revival described by the spectral form factor $K_X(\tau)$ [30,32]. Assuming a normalization $K(\tau \to \infty) \to 1$, the values of the coefficients $a_X = (1, 2, 1)$ and $b_X = (1, 1, 2)$ follow from the requirement that $P_{\mathrm{U}}(\infty) = P_{\mathrm{res}} = \gamma^{-1}$ in the unitary case, and from the above discussion of P_{off} and $P_{\mathrm{pl}}/P_{\mathrm{off}}$. Figure 2(e) shows that this hypothesis is in excellent and parameter-free agreement with our numerical analysis. In each case, a reduction of γ will lead to a rounding of these structures, as we show explicitly for the unitary case [Figs. 2(a)–2(c)].

Applications.—Let us finally mention a few concrete contexts where we expect the above coherent generalization of FGR relaxation dynamics to be physically relevant. The quantum many-body phenomenon that seems to connect most directly to the results of the present Letter is the crossover or transition at the onset of heating in periodically driven (Floquet) systems of finite size [7–9]. Generically, such systems are quantum chaotic both in the nonheating regime and in the regime where they do exchange energy with the periodic drive and thus heat up. The basic decay process in this case changes the system's energy by one quantum of the drive's energy, so a state of the system at one energy decays to states at another energy [7].

Another set of many-body systems where the discreteness of the spectrum of a putative bath plays a central role is the so-called "avalanche" instability of many-body localization in systems with short-range interactions [10–12]. There, a small local rare region serves as a finite bath with a discrete spectrum, and the question is whether this bath succeeds in relaxing distant spins, and thus grows in size or not [33–36]. If the coupling to the bath falls off too rapidly with the distance between the spin and the rare region, the discreteness of the finite bath's spectrum stops its ability to relax spins beyond some finite distance, so the avalanche of thermalization stops and the MBL phase can remain stable [10–12].

A third set of many-body systems where similar considerations arise is in the Fock-space localization description of the onset of many-body quantum chaos in finite-size MBL systems with long-range interactions [13–17], and relatedly, finite-size integrable systems with weak breaking of the integrability [18–20].

Finally, our Letter is also related to previous investigations of the thermalization of finite many-body systems with a single weakly coupled spin [21,22]. In Ref. [21], Crowley and Chandran study deviations from FGR behavior in autocorrelation functions of the weakly coupled spin. In that case the analogous quantum dot model is two weakly coupled dots, each with N levels, which is a different limiting case of the more general two-dot model that we consider in the Supplemental Material [26].

Summary and discussion.—We studied the decay of a quantum state $|0\rangle$ coupled to a system with a large but, importantly, finite dimension N acting as an imperfect bath. Assuming quantum chaos, we modeled the latter by a Gaussian-distributed random matrix of spectral range λ. We analytically calculated the probability $P(t)$ to remain in $|0\rangle$ at time t for the case of weak coupling $g \ll 1$, where the initial state hybridizes with only $\sim\gamma = gN \ll N$ of the bath states. Our main observation is that the decay dynamics is generically nonmonotonic: At early times $\sim(g\lambda)^{-1}$, $P(t)$ decreases to an offset value $P_{\mathrm{off}} \sim 1/(gN)$. This is then followed by a slow process of partial recovery up to a stationary (plateau) value P_{pl}, where the ratio $P_{\mathrm{pl}}/P_{\mathrm{off}} = (2, 3/2, 3)$ is, for $N \gg \gamma \gg 1$, universal and depends only on the symmetry class U, O, or S (broken time reversal, and time-reversal invariant with or without spin rotation symmetry, respectively). We established a quantitative connection between the dynamics of recovery and the spectral form factor of quantum chaos, thus demonstrating that the phenomenon relies on the repulsion of individual levels in the resulting joint level-dot system. This level of sensitivity is remarkable inasmuch as the naive golden rule "smearing" of the initial state over energy $\sim gN$ exceeds the level spacing by far. In the opposite case where only a few levels are coupled $[g \sim O(N^{-1})]$, the decay dynamics is more complicated [Eq. (5)] and effectively described by a washed out version of the form factor. The above phenomena are universal in that they require only relatively mild inducers of quantum chaos. For example, we have checked numerically and analytically that randomly distributed dot-level couplings $\{W_\mu\}$ to a bath of Poisson-distributed levels suffices to generate the above structures. Finally, we have identified a number of examples of genuine many-body dynamics where we expect the phase coherent generalization of Fermi's golden rule introduced in this Letter to become physically important. However, the concrete discussion of how the fundamental physics discussed in this Letter will manifest itself in such applications remains a subject of future research.

D. A. H. was supported in part by NSF QLCI Grant No. OMA-2120757. T. M. acknowledges financial support by Brazilian agencies CNPq and FAPERJ. A. A. acknowledges partial support from the Deutsche Forschungsgemeinschaft (DFG) within the CRC network TR 183 (Project Grant No. 277101999) as part of Projects A03. A. M. was supported in part by the DARPA DRINQS program.

[1] P. A. M. Dirac, The quantum theory of the emission and absorption of radiation, Proc. R. Soc. A **114**, 243 (1927).

[2] J. Orear, E. Fermi, A. Rosenfeld, and R. Schluter, *Nuclear Physics: A Course Given by Enrico Fermi at the University of Chicago*, Midway Reprints (University of Chicago Press, Chicago, 1950).

[3] J. J. Sakurai and J. Napolitano, *Modern Quantum Mechanics*, 2nd ed. (Cambridge University Press, Cambridge, England, 2017).

[4] C. Monroe, W. C. Campbell, L.-M. Duan, Z.-X. Gong, A. V. Gorshkov, P. W. Hess, R. Islam, K. Kim, N. M. Linke, G. Pagano, P. Richerme, C. Senko, and N. Y. Yao, Programmable quantum simulations of spin systems with trapped ions, Rev. Mod. Phys. **93**, 025001 (2021).

[5] J. Preskill, Quantum computing in the NISQ era and beyond, Quantum **2**, 79 (2018).

[6] E. Altman *et al.*, Quantum simulators: Architectures and opportunities, PRX Quantum **2**, 017003 (2021).

[7] A. Morningstar, D. A. Huse, and V. Khemani, Universality classes of thermalization for mesoscopic Floquet systems (to be published).

[8] K. Seetharam, P. Titum, M. Kolodrubetz, and G. Refael, Absence of thermalization in finite isolated interacting Floquet systems, Phys. Rev. B **97**, 014311 (2018).

[9] L. D'Alessio and A. Polkovnikov, Many-body energy localization transition in periodically driven systems, Ann. Phys. (Amsterdam) **333**, 19 (2013).

[10] W. De Roeck and F. Huveneers, Stability and instability towards delocalization in many-body localization systems, Phys. Rev. B **95**, 155129 (2017).

[11] D. J. Luitz, F. Huveneers, and W. De Roeck, How a Small Quantum Bath Can Thermalize Long Localized Chains, Phys. Rev. Lett. **119**, 150602 (2017).

[12] T. Thiery, F. Huveneers, M. Müller, and W. De Roeck, Many-Body Delocalization as a Quantum Avalanche, Phys. Rev. Lett. **121**, 140601 (2018).

[13] B. L. Altshuler, Y. Gefen, A. Kamenev, and L. S. Levitov, Quasiparticle Lifetime in a Finite System: A Nonperturbative Approach, Phys. Rev. Lett. **78**, 2803 (1997).

[14] A. L. Burin, Many-body delocalization in a strongly disordered system with long-range interactions: Finite-size scaling, Phys. Rev. B **91**, 094202 (2015).

[15] K. S. Tikhonov and A. D. Mirlin, Many-body localization transition with power-law interactions: Statistics of eigenstates, Phys. Rev. B **97**, 214205 (2018).

[16] F. Monteiro, T. Micklitz, M. Tezuka, and A. Altland, Minimal model of many-body localization, Phys. Rev. Research **3**, 013023 (2021).

[17] F. Monteiro, M. Tezuka, A. Altland, D. A. Huse, and T. Micklitz, Quantum Ergodicity in the Many-Body Localization Problem, Phys. Rev. Lett. **127**, 030601 (2021).

[18] V. B. Bulchandani, D. A. Huse, and S. Gopalakrishnan, Onset of many-body quantum chaos due to breaking integrability, Phys. Rev. B **105**, 214308 (2022).

[19] D. A. Rabson, B. N. Narozhny, and A. J. Millis, Crossover from poisson to Wigner-Dyson level statistics in spin chains with integrability breaking, Phys. Rev. B **69**, 054403 (2004).

[20] M. Žnidarič, Weak Integrability Breaking: Chaos with Integrability Signature in Coherent Diffusion, Phys. Rev. Lett. **125**, 180605 (2020).

[21] P. J. D. Crowley and A. Chandran, Partial thermalisation of a two-state system coupled to a finite quantum bath, SciPost Phys. **12**, 103 (2022).

[22] D. Sels and A. Polkovnikov, Thermalization of dilute impurities in one dimensional spin chains, arXiv:2105.09348.

[23] P. W. Milonni, J. R. Ackerhalt, H. W. Galbraith, and M.-L. Shih, Exponential decay, recurrences, and quantum-mechanical spreading in a quasicontinuum model, Phys. Rev. A **28**, 32 (1982).

[24] J. H. Eberly, N. B. Narozhny, and J. J. Sanchez-Mondragon, Periodic Spontaneous Collapse and Revival in a Simple Quantum Model, Phys. Rev. Lett. **44**, 1323 (1980).

[25] P. A. Mello, P. Pereyra, and N. Kumar, A soluble random-matrix model for relaxation in quantum systems, J. Stat. Phys. **51**, 77 (1988).

[26] See Supplemental Material at http://link.aps.org/supplemental/10.1103/PhysRevLett.129.140402 for details on the calculation of P_{res} and a summary of the spectral form factor for the three Wigner-Dyson classes, which includes Ref. [24].

[27] A. D. Mirlin, Statistics of energy levels and eigenfunctions in disordered systems, Phys. Rep. **326**, 259 (2000).

[28] G. Livan, M. Novaes, and P. Vivo, *Introduction to Random Matrices* (Springer International Publishing, New York, 2018).
[29] Equation (4) requires an O(1) correction factor as $\gamma \to N$ for finite N because of the nonuniform density of states of the dot. However, we focus on $\gamma \ll N$ in this Letter.
[30] J. Liu, Spectral form factors and late time quantum chaos, Phys. Rev. D **98**, 086026 (2018).
[31] K. Efetov, *Supersymmetry in Disorder and Chaos* (Cambridge University Press, Cambridge, England, 1999).
[32] F. Haake, *Quantum Signatures of Chaos* (Springer-Verlag, Berlin, 2006).
[33] P. J. D. Crowley and A. Chandran, Avalanche induced coexisting localized and thermal regions in disordered chains, Phys. Rev. Research **2**, 033262 (2020).
[34] I.-D. Potirniche, S. Banerjee, and E. Altman, Exploration of the stability of many-body localization in $d > 1$, Phys. Rev. B **99**, 205149 (2019).
[35] M. Goihl, J. Eisert, and C. Krumnow, Exploration of the stability of many-body localized systems in the presence of a small bath, Phys. Rev. B **99**, 195145 (2019).
[36] J. Léonard, M. Rispoli, A. Lukin, R. Schittko, S. Kim, J. Kwan, D. Sels, E. Demler, and M. Greiner, Signatures of bath-induced quantum avalanches in a many-body–localized system, arXiv:2012.15270.